



ELSEVIER

journal homepage: [www.elsevier.com/locate/febsopenbio](http://www.elsevier.com/locate/febsopenbio)

## Biophysical analysis of the interaction of the serum protein human $\beta_2$ GPI with bacterial lipopolysaccharide

Anna Gries<sup>a,\*</sup>, Ruth Prassl<sup>b</sup>, Satoshi Fukuoka<sup>c</sup>, Manfred Rössle<sup>d</sup>, Yani Kaconis<sup>e</sup>, Lena Heinbockel<sup>e</sup>, Thomas Gutschmann<sup>e</sup>, Klaus Brandenburg<sup>e</sup>

<sup>a</sup>Institute of Physiology, Medical University of Graz, Harrachgasse 21/V, 8010 Graz, Austria

<sup>b</sup>Institute of Biophysics, Medical University of Graz, Schmiedlstr. 6, 8042 Graz, Austria

<sup>c</sup>National Institute of Advanced Industrial Science and Technology AIST, Takamatsu, Japan

<sup>d</sup>European Molecular Biology Laboratory, c/o DESY, D-22603 Hamburg, Germany

<sup>e</sup>Forschungszentrum Borstel, Leibniz-Zentrum für Medizin und Biowissenschaften, Parkallee 10, D-23845 Borstel, Germany

### ARTICLE INFO

#### Article history:

Received 7 February 2014

Revised 23 April 2014

Accepted 23 April 2014

#### Keywords:

Human glycoprotein  $\beta_2$ GPI

Lipopolysaccharide

Cytokine production

Immune modulation

LAL test

### ABSTRACT

There are several human serum proteins for which no clear role is yet known. Among these is the abundant serum protein beta2-glycoprotein-I ( $\beta_2$ GPI), which is known to bind to negatively charged phospholipids as well as to bacterial lipopolysaccharides (LPS), and was therefore proposed to play a role in the immune response. To understand the details of these interactions, a biophysical analysis of the binding of  $\beta_2$ GPI to LPS and phosphatidylserine (PS) was performed. The data indicate only a moderate tendency of the protein (1) to influence the LPS-induced cytokine production *in vitro*, (2) to react exothermally with LPS in a non-saturable way, and (3) to change its local microenvironment upon LPS association. Additionally, we found that the protein binds more strongly to phosphatidylserine (PS) than to LPS. Furthermore,  $\beta_2$ GPI converts the LPS bilayer aggregates into a stronger multilamellar form, and reduces the fluidity of the hydrocarbon moiety of LPS due to a rigidification of the acyl chains. From these data it can be concluded that  $\beta_2$ GPI plays a role as an immune-modulating agent, but there is much less evidence for a role in immune defense against bacterial toxins such as LPS.

© 2014 The Authors. Published by Elsevier B.V. on behalf of the Federation of European Biochemical Societies. This is an open access article under the CC BY-NC-ND license (<http://creativecommons.org/licenses/by-nc-nd/3.0/>).

### 1. Introduction

Serum proteins such as albumin or low- and high-density lipoproteins (LDL and HDL) fulfill a variety of physiological tasks like transport, adhesion, recognition and defenses against invading microorganisms. To this class also belong lipopolysaccharide-binding protein (LBP) and lactoferrin which are considerably up-regulated in acute phase serum i.e. in the case of bacterial infections [1,2]. In contrast the function of the abundant serum protein  $\beta_2$ GPI is not completely understood. Various publications presented data on its role as binding molecule to acidic lipids. Actually

*Abbreviations:*  $\beta_2$ GPI, beta2-glycoprotein-I; FRET, fluorescence resonance energy transfer spectroscopy; FTIR, Fourier-transform infrared spectroscopy; HDL, high-density lipoproteins; ITC, isothermal titration calorimetry; LAL, Limulus amoebocyte lysate; LBP, lipopolysaccharide-binding protein; LDL, low-density lipoproteins; LPS, lipopolysaccharides; MNC, mononuclear cells; PC, phosphatidylcholine; PS, phosphatidylserine; SAXS, small-angle X-ray scattering

\* Corresponding author. Tel.: +43 3163804492.

E-mail address: [anna.gries@medunigraz.at](mailto:anna.gries@medunigraz.at) (A. Gries).

the analysis of the crystal structure of  $\beta_2$ GPI [3,4] gave evidence for domain V being an excellent counterpart for negatively charged phospholipids. These data were extended by Hammel et al. [5] who found a direct interaction of acidic phospholipids such as cardiolipin with the hydrophobic loop adjacent to the positively charged lysine-rich region of domain V of  $\beta_2$ GPI.

There is some evidence that  $\beta_2$ GPI may also play a role as regulator of the immune response to bacterial toxins such as lipopolysaccharide (LPS, endotoxin). Laplante and co-workers published data giving evidence that  $\beta_2$ GPI interacts specifically with LPS and that both LPS and Toll-like receptor 4 (TLR4) are required for  $\beta_2$ GPI to activate macrophages [6]. This idea was even more expressed in the investigations of Agar et al. [7] who proposed that  $\beta_2$ GPI might be a scavenger of LPS deduced from the inhibition of the LPS-induced expression of tissue factor and interleukin-6 (IL-6) from monocytes.

From these findings the role of  $\beta_2$ GPI still does not seem to be clear. Therefore, we have applied various biophysical techniques to study the interaction of  $\beta_2$ GPI with LPS in more detail. This is

<http://dx.doi.org/10.1016/j.fob.2014.04.008>

2211-5463/© 2014 The Authors. Published by Elsevier B.V. on behalf of the Federation of European Biochemical Societies. This is an open access article under the CC BY-NC-ND license (<http://creativecommons.org/licenses/by-nc-nd/3.0/>).

of special importance since LPS belongs to the strongest elicitors of the immune system known in nature. It is responsible, for example, for the induction of many cytokines and chemokines but also for the production of prostaglandins in human mononuclear cells [8]. These induction mechanisms may be beneficial at low amounts of LPS but lead to pathophysiological reactions at higher LPS concentrations such as the induction of sepsis. Although  $\beta_2$ GPI binds to LPS we did not get evidence for a significant role of  $\beta_2$ GPI as defense protein. We propose rather an activity-modulating role possibly in the sense of an immune modulation which may be important to combat LPS-induced inflammation by enhancing the innate immunity.

## 2. Materials and methods

### 2.1. Lipopolysaccharide and $\beta_2$ GPI

Lipopolysaccharides from *Salmonella enterica* Minnesota rough mutants Re and Ra, strains R595 and R60 were extracted from the bacteria grown at 37 °C by the phenol:chloroform:petrol ether (PCP) method, purified and used in the natural salt form [9]. The purity was examined by MALDI-TOF mass spectrometry and LPS samples were only used when the chemical structure in particular of the lipid A part consisted of a diglucosamine to which six acyl chains in amide- and ester-linkage at positions 2 and 2', and 3 and 3', respectively, were bound and which were phosphorylated at positions 1 and 4', according to the known structure of lipid A.

LPS Re and Ra were either dissolved in 50 mM Tris-HCl, 25 mM NaCl, 0.1 g/L EDTA, pH 7.4 (Tris-HCl) or in 20 mM Hepes buffer at concentrations of 1 mg/ml. The samples were sonicated for 20 min at 60 °C followed by 30 min cooling to 4 °C and afterwards reheated to 60 °C for 30 min and finally stored at 4 °C for at least 12 h before use.

### 2.2. Phospholipids

Egg yolk phosphatidylcholine (Egg-PC) or phosphatidylserine (PS) purchased from Avanti Polar Lipids (Alabaster, USA) were dissolved in chloroform/methanol 2:1 (v/v). The organic solvents were evaporated at 40 °C under a stream of nitrogen. The film was dried in high vacuum overnight to remove residual traces of solvent. The dry lipid film (1 mg lipid) was suspended in 1 ml Tris-HCl and hydrated at 50 °C for 1 h interrupted by vigorous mixing every 10 min. Lipid suspensions were extruded through a polycarbonate filter with 100 nm pore size using a LiposoFast pneumatic extruder (Avestin, Inc. Ottawa, ON).

### 2.3. Isolation of beta2-glycoprotein-I

$\beta_2$ GPI was purified from human plasma by treatment with 1.4% (v/v) perchloric acid followed by affinity chromatography on heparin-sepharose and cation exchange chromatography on Mono S (Pharmacia, Sweden) [10]. The preparation was homogenous as judged by SDS/PAGE (10% resolving and 3.75% stacking gel) yielding a single band.

### 2.4. Intrinsic Trp-fluorescence

Trp-fluorescence was recorded on a Spex Fluoromax-3 fluorescence spectrometer (Jobin Yvon Horiba, Longjumeau, France) using a 10 mm × 10 mm quartz cuvette. Trp-residues were excited at 292 nm and emission spectra were recorded from 320 to 380 nm with an increment of 1 nm. Band widths of 5 nm were used for excitation and emission with an integration time of 0.1 s, averaging 10 scans. The emission scans were processed for inner filter and

instrumental corrections and the background intensities of the samples without protein were subtracted. Titration experiments were performed with continuous stirring by adding aliquots of LPS (0.5 mg/ml suspended in Tris-HCl) into the cuvette containing  $\beta_2$ GPI (50  $\mu$ g/ml, 1.1  $\mu$ M) dissolved in the same buffer. The ratio of LPS/ $\beta_2$ GPI was incrementally increased from 0 to 40 mol/mol by titration. Control experiments were performed in the same way by adding aliquots of Egg-PC unilamellar vesicles.

The temperature of the cuvette was maintained at 25 °C and the single measurements were taken after 10 min of equilibration.

### 2.5. Acrylamide quenching of Trp fluorescence

Aliquots of a 3 M acrylamide stock solution in Tris-HCl were added to a 1.1  $\mu$ M solution of  $\beta_2$ GPI containing 20 mol LPS/mol protein. The acrylamide concentration was varied in a range between 0.02 and 0.45 M. The experimental conditions were as described above. The values obtained were corrected for volume increase and scattering derived from acrylamide titration of LPS.

The fluorescence quenching data were analyzed with a Stern-Volmer plot. In the case where both static and dynamic quenching occur simultaneously in the sample the following modified form of the Stern-Volmer equation holds

$$I_0/I = (1 + K_{sv}[Q])\exp^{V/Q}$$

where  $I_0$  is the fluorescence intensity at zero quencher concentration,  $I$  is the maximum intensity at a given quencher concentration  $[Q]$ , and  $K_{sv}$  is the Stern-Volmer quenching constant. The term  $\exp(V/Q)$  is used as a phenomenological descriptor of the quenching process where  $V$  represents an active volume of a sphere around the fluorophore to such an extent that any quencher within this volume is able to quench the excited fluorophore at the time of fluorophore excitation.

### 2.6. Stimulation of human mononuclear cells by LPS

The stimulation of human mononuclear cells (MNC) was performed as described previously [11]. Briefly MNC were isolated from heparinized blood of healthy donors. The cells were resuspended in medium (RPMI 1640) at  $5 \times 10^6$  cells/ml. For stimulation 200  $\mu$ l MNC ( $1 \times 10^6$  cells) were transferred into each well of a 96-well culture plate. LPS Ra and  $\beta_2$ GPI mixtures were preincubated for 30 min at 37 °C and added to the cultures at 20  $\mu$ l per well. The cultures were incubated for 4 h at 37 °C under 5% CO<sub>2</sub>. After centrifugation of the culture plates for 10 min at 400g supernatants were collected and stored at -20 °C. TNF $\alpha$  concentrations were quantified by a sandwich ELISA using a monoclonal antibody against TNF (clone 6b from Intex AG, Switzerland).

### 2.7. X-ray scattering

The aggregate structures of LPS Ra were determined in the absence and presence of  $\beta_2$ GPI using small-angle X-ray scattering (SAXS). SAXS measurements were performed at the European Molecular Biology Laboratory (EMBL) outstation at the Hamburg synchrotron radiation facility HASYLAB using the double-focusing monochromator-mirror camera X33. Scattering patterns in the range of the scattering vector  $0.01 < s < 0.1 \text{ nm}^{-1}$  ( $s = 2 \sin \theta / \lambda$ ,  $2\theta$  scattering angle and  $\lambda$  the wavelength = 0.15 nm) were recorded at 20, 40, 60, and 80 °C with exposure times of 1 min using an image plate detector with online readout (MAR345, MarResearch, Norderstedt/Germany) [12]. The  $s$ -axis was calibrated with Ag-Behenate with a periodicity of 5.84 nm. The scattering patterns were evaluated as described previously [13] assigning the spacing ratios of the main scattering maxima to defined three-dimensional

structures. The lamellar and cubic structures are most relevant in the present study.

### 2.8. Fourier-transform infrared spectroscopy (FTIR)

FTIR was used to determine (a) the gel to liquid crystalline phase transition of the hydrocarbon chains of LPS by evaluating the peak position of the symmetric stretching vibration  $\nu_s(\text{CH}_2)$  in the wavenumber range 2850–2853  $\text{cm}^{-1}$  and (b) the secondary structure of the protein in the range of the amide I vibration in the wavenumber range 1700–1600  $\text{cm}^{-1}$  [14,15]. The infrared spectroscopic measurements were performed on an IFS-55 spectrometer (Bruker). LPS and LPS: $\beta_2$ GPI samples dispersed in 20 mM Hepes buffer, pH 7.0 were placed in a  $\text{CaF}_2$  cuvette between two 12.5  $\mu\text{m}$  teflon spacers. For the determination of the phase behavior temperature-scans were performed automatically between 10 and 70 °C with a heating-rate of 0.6 °C/min. Every 3 °C, 50 interferograms were accumulated, apodized, Fourier transformed and converted to absorbance spectra. For the determination of the secondary structures an attenuated total reflection unit was used whereupon the protein and protein:LPS mixtures were spread under evaporation of the excess water in a stream of nitrogen and measuring the samples at the temperature of the instrument (30 °C).

### 2.9. Isothermal titration calorimetry (ITC)

Microcalorimetric measurements of the binding of  $\beta_2$ GPI to LPS Ra were performed on an MCS isothermal titration calorimeter (Microcal Inc.) at 37 °C as described previously [13]. LPS Ra (0.05 mM) was dispensed into the microcalorimetric cell (volume 1.3 ml) and the protein solution (1 mM) was filled into the syringe compartment (volume 100  $\mu\text{l}$ ). After temperature equilibration  $\beta_2$ GPI was titrated every 5 min in 3  $\mu\text{l}$  portions into the LPS-containing cell under constant stirring and the heat of reaction was plotted versus time.

### 2.10. Fluorescence resonance energy transfer spectroscopy (FRET)

The ability of  $\beta_2$ GPI to bind to and intercalate into phospholipid liposomes or into LPS R60 aggregates was investigated by FRET as described earlier [13]. Briefly, phospholipid liposomes from phosphatidylserine (PS), phosphatidylcholine (PC) or LPS R60 were doubly labeled with the fluorescent phospholipid dyes N-(7-nitrobenz-2-oxa-1,3-diazol-4yl)-phosphatidyl ethanolamine (NBD-PE) and N-(lissamine rhodamine B sulfonyl)-phosphatidylethanolamine (Rh-PE) (Molecular Probes). Intercalation of unlabeled molecules into the doubly labeled liposomes leads to probe dilution and thereby to a lower FRET efficiency. Thereby the emission intensity of the donor  $I_D$  increases and that of the acceptor  $I_A$  decreases (for clarity, only the quotient of the donor and acceptor emission intensity is shown here).

In all experiments 100  $\mu\text{l}$  of 100  $\mu\text{M}$   $\beta_2$ GPI were added to doubly labeled PC, PS or LPS R60 (900  $\mu\text{l}$  of 10  $\mu\text{M}$ ) at 50 s after equilibration. NBD-PE was excited at 470 nm and the donor and acceptor fluorescence intensities were monitored at 531 and 593 nm respectively and the fluorescence signal  $I_D/I_A$  was recorded for further 250 s.

### 2.11. Determination of endotoxin activity by the chromogenic Limulus test

To test a possible contamination of  $\beta_2$ GPI with endotoxins the LPS content was determined by a quantitative kinetic assay based on the reactivity of Gram-negative endotoxin with Limulus ameobocyte lysate (LAL) at 37 °C, using test kits of LAL Coamatic

Chromo-LAL K (Chromogenix, Haemochrom). The standard endotoxin used in this test was from *Escherichia coli* (O55:B5) and 10–15 endotoxin units (EU)/ml correspond to 1 ng/ml. In this assay saturation occurs at 50 EU/ml and the resolution limit is 0.05 EU/ml (maximum value for ultrapure water, Aqua B. Braun).

## 3. Results

### 3.1. Purity of $\beta_2$ GPI

Despite the extraction and purification procedure leading to a single band in SDS-PAGE as described above contamination by LPS cannot be excluded. Therefore endotoxin was determined in the Limulus ameobocyte lysate (LAL) assay and the results are shown in Table 1. Clearly the protein is not free of LPS. From the data of Table 1 an endotoxin concentration of  $\sim 2$  EU/ $\mu\text{g}$  can be estimated which corresponds to approximately 150–250 pg LPS per  $\mu\text{g}$  protein.

### 3.2. Stimulation of mononuclear cells

Serum proteins such as  $\beta_2$ GPI are important LPS binding proteins. Therefore the ability of  $\beta_2$ GPI to influence the inflammation induction by LPS was investigated by stimulating mononuclear cells (MNC) with LPS at different concentrations (100 and 10 ng/ml) in the absence and presence of varying concentrations of  $\beta_2$ GPI ([LPS]:[ $\beta_2$ GPI] 1:1, 1:10, 1:100, and 1:1000 weight%). The addition of the protein to LPS at a ratio of 1:1 and 1:10 respectively influenced the LPS-induced cytokine (TNF $\alpha$ ) secretion only marginally (data not shown). At ratios of 1:100 and 1:1000 however a clear

**Table 1**

Limulus assay of pure  $\beta_2$ GPI. In the LAL assay a concentration of 1 ng/ml LPS corresponds to 10–15 EU/ml. From these data, a medium LPS content of 2 EU/ $\mu\text{g}$  can be estimated.

c( $\beta_2$ GPI) [ $\mu\text{g}/\text{ml}$ ]	Dilution	LAL result (diluted) [EU/ml]	LAL result (undiluted) [EU/ml]	App. LPS-content [EU/ $\mu\text{g}$ ]
800	1	1863.3	1863.3	2.3
80	10	152.99	1529.9	1.9
8	100	14.641	1466.41	1.8

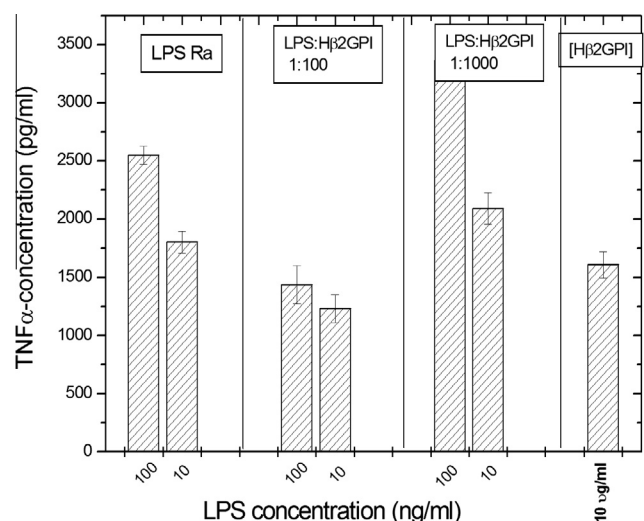


**Fig. 1.** Secretion of tumor-necrosis-factor $\alpha$  from human mononuclear cells induced by lipopolysaccharide LPS Ra, and LPS: $\beta_2$ GPI mixtures. The error bar results from the determination of TNF $\alpha$  in an ELISA in duplicate.

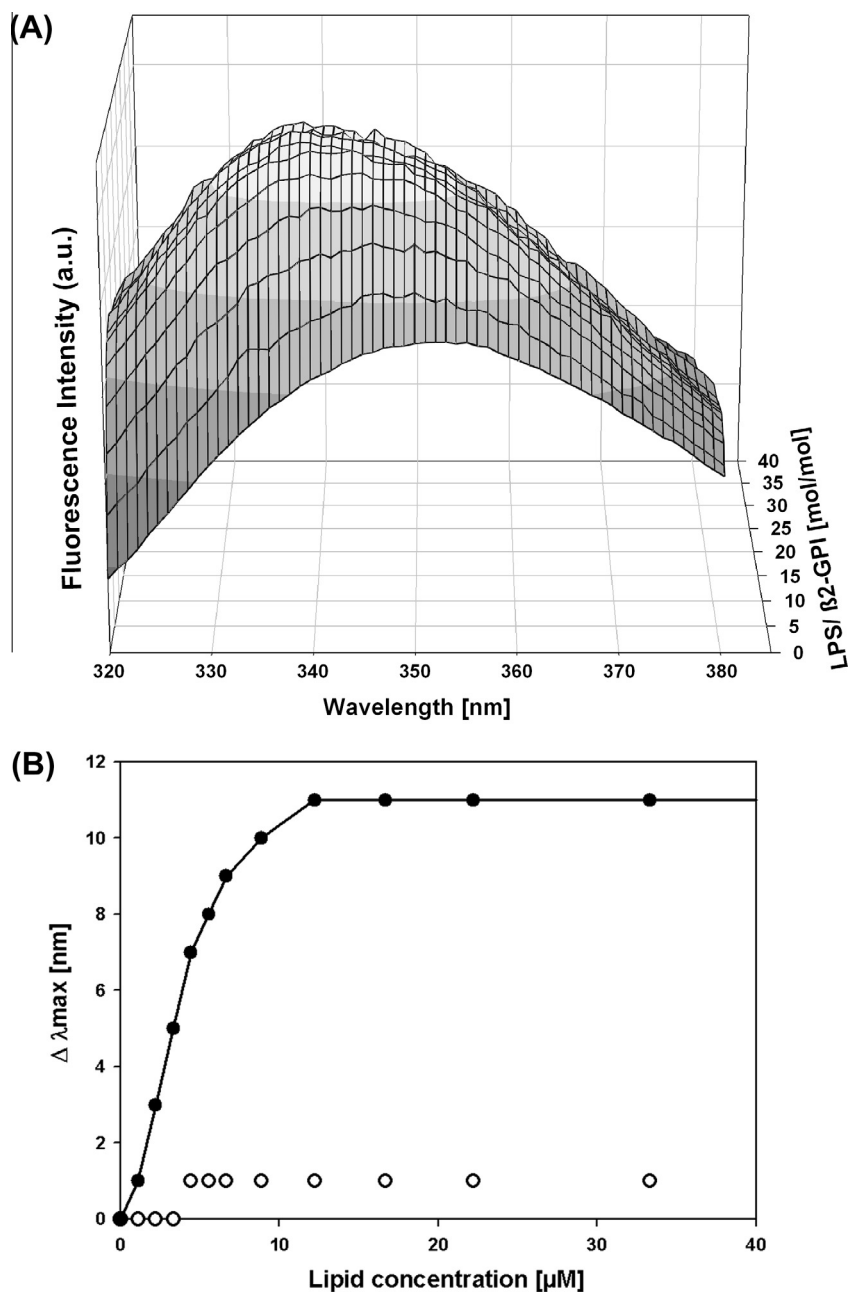


**Fig. 2.** (A) Trp-fluorescence emission spectra of  $\beta_2$ GPI/LPS at a protein concentration of 1.1  $\mu$ M and in the presence of increasing concentrations of LPS varying from 0 to 40 mol LPS/mol protein. Excitation wavelength was 292 nm. The results are presented in a mesh plot. (B) Changes in the emission maximum of Trp-fluorescence of  $\beta_2$ GPI (1.1  $\mu$ M) in the presence of lipid vesicles as a function of lipid concentration for LPS (●) and egg-PC (○).

change of the cytokine secretion was observed (Fig. 1). TNF $\alpha$  concentrations in the range 2000–1750 pg/ml for pure LPS are significantly reduced at [LPS]:[ $\beta_2$ GPI] 1:100. Interestingly there is no further decrease at the highest concentration. In contrary, at [LPS]:[ $\beta_2$ GPI] 1:1000 a highly significant increase of TNF $\alpha$  secretion can be observed. The bar at the right hand side in Fig. 1 shows that the protein itself seems to be an activator of MNC. This activity however could be explained at least partially by the presence of LPS inasmuch as 10  $\mu$ g/ml  $\beta_2$ GPI were contaminated by 2 ng/ml LPS.

### 3.3. Interaction of $\beta_2$ GPI with LPS-aggregates assessed by Intrinsic Trp-fluorescence

Interaction of  $\beta_2$ GPI with LPS was monitored by measuring alterations in the fluorescence spectra of tryptophan (Trp), which

occur due to changes in the microenvironment of Trp-residues. As shown in our previous paper on the binding behavior of  $\beta_2$ GPI to negatively charged cardiolipin vesicles [5], the Trp-emission spectrum of  $\beta_2$ GPI is rather broad with a maximum ( $\lambda_{max}$ ) at about 350 nm. This feature arises by reason of different microenvironments of the five Trp-residues in  $\beta_2$ GPI. Four Trp-residues located in domain 1–4 are embedded in the interior hardly accessible to water whereas Trp316 located in domain V is surface exposed [3]. Despite its apolar nature Trp316 is positioned in a hydrophobic loop which is surface exposed and was found to be essential for the lipid-binding capacity of  $\beta_2$ GPI, as a single point mutation of this amino acid completely abrogates lipid binding [16,17]. Thus one can assume that upon lipid association Trp316 becomes located in a more hydrophobic lipid environment seen as a blue shift in the fluorescence emission spectra. Indeed a significant blue shift



from 350 nm to 336 nm was observed when cardiolipin vesicles were added to a solution of  $\beta_2$ GPI. The magnitude of the blue shift was dependent on the molar ratio of lipid-to-protein being constant above a molar ratio of 20 mol lipid per mol protein [5].

Here we have performed an analogous experiment applying increasing LPS concentrations between 0 and 45  $\mu$ M corresponding to molar ratios up to 40 mol LPS/mol  $\beta_2$ GPI. Depending on the concentration of LPS a blue shift from 350 nm to 339 nm was observed which in contrast to cardiolipin increases linearly up to 5  $\mu$ M LPS and remains unchanged above a molar ratio of about 10 (Fig. 2A and B). As  $\beta_2$ GPI lacks the ability to bind to zwitterionic choline headgroups [5,18], the fluorescence emission maximum observed for egg-PC at 350 nm remained unchanged (Fig. 2B).

Fig. 3 shows the Stern–Vollmer plots for the quenching of the intrinsic Trp fluorescence by acrylamide. We observed a non-linear biphasic characteristic of the quenching curves with an upward curvature indicative for simultaneous static and dynamic quenching. The effective quenching constants were determined from the exponential fit as  $K_{sv} = 4.5 \text{ M}^{-1}$  and  $3.2 \text{ M}^{-1}$  for  $\beta_2$ GPI and  $\beta_2$ GPI/LPS, respectively. The lower quenching rate for  $\beta_2$ GPI/LPS indicates a lower accessibility of Trp-residues to polar quencher in presence of LPS however the effect is much less pronounced as reported for cardiolipin [5].

### 3.4. Gel to liquid crystalline phase transition of the acyl chains of LPS

The gel ( $\beta$ ) to liquid crystalline ( $\alpha$ ) phase transition of LPS ranges from 30 to 35  $^{\circ}\text{C}$  for enterobacterial LPS. Binding to serum proteins may play a role in modulating immune responses to LPS. In Fig. 4, in FTIR experiments as sensitive indicator of the phases the peak position of the symmetric stretching vibration at 2850–2853  $\text{cm}^{-1}$  is plotted for pure LPS as well as in the presence of  $\beta_2$ GPI at a ratio of [LPS]:[ $\beta_2$ GPI] 1:1 weight%. For LPS alone the wavenumber values changed from 2850.5 to 2852.5–2853.0  $\text{cm}^{-1}$  indicating a midpoint of the transition at 32.4  $^{\circ}\text{C}$  which considerably increased to a value of 36.3  $^{\circ}\text{C}$  in the presence of [LPS]:[ $\beta_2$ GPI] 1:1 weight%. At the same time, at all temperatures the wavenumber values are lower for the sample with protein. Both effects shift in  $T_m$  to higher values as well as decrease in wavenumbers are characteristic for a rigidification of the entire LPS aggregate.

### 3.5. Secondary structure of $\beta_2$ GPI

The secondary structures of proteins such as  $\alpha$ -helical and  $\beta$ -sheets and their changes due to interaction with LPS may be of relevance for an understanding of the mode of action. FTIR allows an analysis of the secondary structures by evaluating the amide I vibration in the spectral range of 1700–1600  $\text{cm}^{-1}$ . The main secondary structural elements  $\alpha$ -helix,  $\beta$ -sheets, and random coils have maxima at 1650–1657, 1625–1640, and 1645–1660  $\text{cm}^{-1}$ , respectively. A particular helical substructure,  $3_{10}$  helices, has bands around 1637–1643  $\text{cm}^{-1}$ .

In Fig. 5, data are presented for pure  $\beta_2$ GPI and in the presence of LPS ([LPS]:[ $\beta_2$ GPI] 10:1). The pure protein exhibits a main vibrational maximum at 1640.7  $\text{cm}^{-1}$ , which is shifted to a value of 1648.4  $\text{cm}^{-1}$  in the presence of LPS. The position of the former band may indicate a mixture of a  $\beta$ -sheet and a  $3_{10}$  helical structure. In the presence of LPS the significant shift to higher wavenumbers is indicative for a transformation, at least partially, into a random coil organization. Since the assignment to the different secondary structures may be difficult due to the superposition of the single band components we have also applied resolution-enhancing techniques such as Fourier self-deconvolution (FSD) and second derivatives of the spectra, but these analyzes did not provide any extra support for an increase in random structure.

### 3.6. Three-dimensional aggregate structure of LPS

The supramolecular aggregate structure of LPS has been shown to represent an important determinant for its ability to be biologically active i.e. by inducing the cytokine production in human MNC. Changes of the aggregate structure due to protein binding may strongly influence the capability of LPS to induce cytokines.

The determination of the aggregate structure can be performed by SAXS which shows characteristic scattering patterns depending on the kind of aggregates. For pure LPS the scattering patterns exhibit broad intensity distributions between  $s$  values of 0.15–0.35  $\text{nm}^{-1}$  indicating the existence of LPS bilayer systems (form factor), which do not show a particular aggregation behavior (no structure factor), in accordance to numerous data published earlier [19].

In the presence of the protein ([LPS]:[ $\beta_2$ GPI] 1:4) the scattering patterns in the range of 20–80  $^{\circ}\text{C}$  (Fig. 6) exhibit sharp reflections

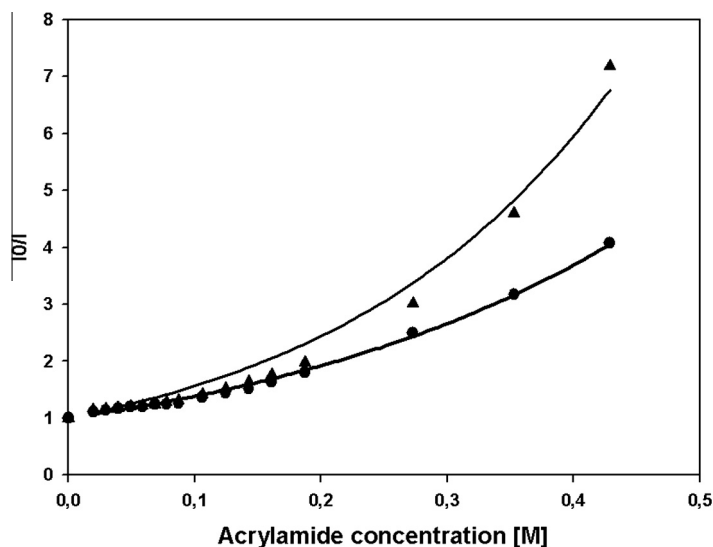
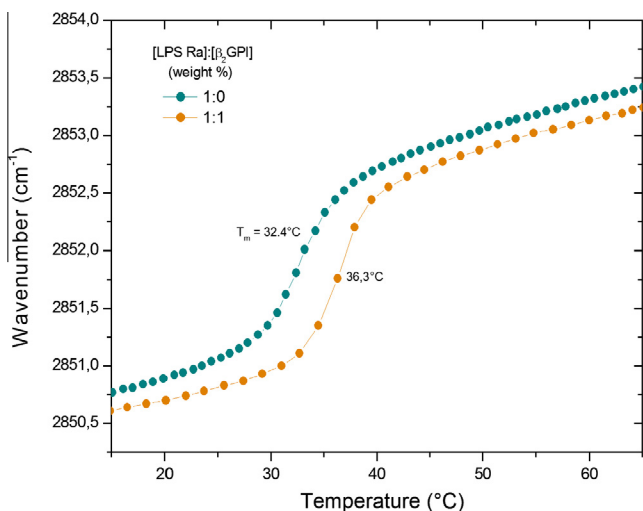
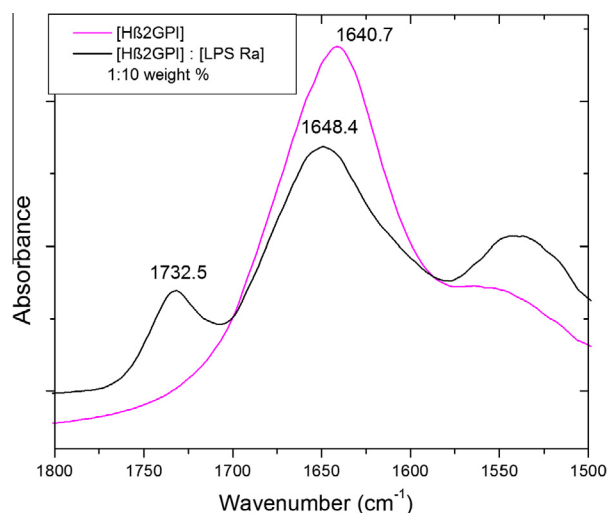


Fig. 3. Quenching of the intrinsic Trp fluorescence of  $\beta_2$ GPI by acrylamide. The protein concentration was set to 1.1  $\mu$ M. The acrylamide concentration was increased to 0.45 M. The Stern–Vollmer plot is shown for  $\beta_2$ GPI in the absence (▲) and in the presence of 20 mol LPS/mol protein (●).



**Fig. 4.** Gel to liquid crystalline phase transition of the acyl chains of LPS Ra in the absence and presence of  $\beta_2$ GPI at [LPS]:[ $\beta_2$ GPI] 10:1 weight%. Shown is the peak position of the symmetric stretching vibration of the methylene groups  $\nu_s(\text{CH}_2)$  versus temperature. In the gel phase, the position lies around 2850.5, in the liquid crystalline phase at 2852.5–2853  $\text{cm}^{-1}$ .



**Fig. 5.** Infrared vibrational spectra in the range of the amide I band (predominantly C=O stretching vibration). The position of the peak maxima can be assigned to different secondary structures due to different water binding, i.e.,  $\alpha$ -helix between 1650 and 1655  $\text{cm}^{-1}$ ,  $\beta$ -sheets between 1625 and 1640  $\text{cm}^{-1}$ , and a particular helical structure  $3_{10}$ -helix between 1637 and 1643  $\text{cm}^{-1}$ .

with one main reflection  $d_1$  and the second order at  $d_1/2$ , at 80 °C also with the third order reflection at  $d_1/3$ . This behavior can be interpreted as occurrence of a multilamellar LPS aggregate due to protein binding with a lamellar periodicity of 9.12–8.77 nm generated i.e. by distances between neighboring bilayer planes. However from the sharpness of the single reflections it can be deduced that the multilamellarization is only weakly expressed.

### 3.7. Thermodynamics of binding of $\beta_2$ GPI to lipopolysaccharide

Isothermal titration calorimetry (ITC) is an important technique to study the thermodynamics of molecule interactions. In this way characteristics of binding (endotherm, exotherm), the binding stoichiometry and saturation can be analyzed.

Data presented in Fig. 7 indicate an exclusively exothermic process, which however does not show a sigmoidal saturation profile as normally observed in this type of measurement. A sigmoidal response is not necessarily to be expected in the case of specific interactions, in particular for binding proteins such as lactoferrin. It was not possible over the range of [protein]:[LPS] ratios used here to evaluate binding constants. Furthermore, the observed small enthalpy changes in the range  $-8$  to  $-2$  kJ/mol indicate only a weak binding of the protein to LPS.

### 3.8. Intercalation of $\beta_2$ GPI into phospholipids or LPS

FRET was applied to study a possible intercalation of  $\beta_2$ GPI into phospholipid liposomes made from PC or PS or into LPS aggregates. As shown in Fig. 8A–C there is only a very weak interaction of  $\beta_2$ GPI with PC (Fig. 8A) leading to an insignificant change of the FRET signal of 0.02. For the interaction of  $\beta_2$ GPI with the negatively charged phospholipid PS there is a much higher change of the FRET signal of nearly 0.2 (Fig. 8B). Despite the highly negative head group charge of LPS the interaction with  $\beta_2$ GPI leads to an increase of the FRET of only 0.05 (Fig. 8C).

## 4. Discussion

We have performed a biophysical analysis of the abundant serum protein  $\beta_2$ GPI with bacterial lipopolysaccharides and in some cases also with phospholipids to understand the still insufficiently defined role of  $\beta_2$ GPI. We have found that  $\beta_2$ GPI provokes an increase in the phase transition temperature of LPS (Fig. 4). Additionally a change of the aggregate structure of LPS with a moderate tendency to aggregate into a multilamellar phase was observed (Fig. 6). At the same time the interaction indicates a clearly exothermic process (Fig. 7) which, however, shows no saturation characteristics. This is in accordance with the rather weak interaction in the FRET experiment (Fig. 8C) being lower than that with the negatively charged PS (Fig. 8A), despite the fact that the surface charge density of PS is lower than that of LPS. Concomitantly to these physical data the biological experiment exhibits a moderate decrease of the LPS-induced stimulation of human mononuclear cells (Fig. 1) in a concentration range ([LPS]:[ $\beta_2$ GPI] 1:1–1:100) in which the endotoxin contaminant within the  $\beta_2$ GPI does not yet play a role.

The experimental data of the secondary structures of the protein (Fig. 5) are indicative of a slight transformation of the  $\beta$ -sheet and a  $3_{10}$  helical structure of the protein into – as one possible interpretation – a random coil conformation. Literature data of secondary structures of  $\beta_2$ GPI have been published by Paolorossi and Montich [20] and Borchman et al. [21]. The former group found – among others – a temperature-dependent distribution of  $\beta$ -sheets (bands at 1631–1636  $\text{cm}^{-1}$ ) and  $\alpha$ -helical structures with the former structures dominant at 25 °C and the latter at 50 °C. In the presence of negatively charged phosphatidylglycerols (POPG, DMPG, DPPG), the main components at 1631–1633  $\text{cm}^{-1}$  remained corresponding to  $\beta$ -sheets but may be influenced by the addition of NaCl leading partially to more  $\alpha$ -helical structures. The data of Borchman et al. [21] show significant variations already for different preparations of the protein with 27 and 39%  $\alpha$ -helix and  $\beta$ -sheets for one and 36 and 53% respectively for the other. Also the turns vary considerably while no random coil structures were observed. In the presence of phosphatidylcholine the structural units corresponding to turns nearly disappeared whereas the addition of the negatively charged cardiolipin led to a significant increase of random coil structures. This phenomenon was also observed in this work after addition of LPS. Summarizing the different data and interpretations in the literature and observed in our experiments

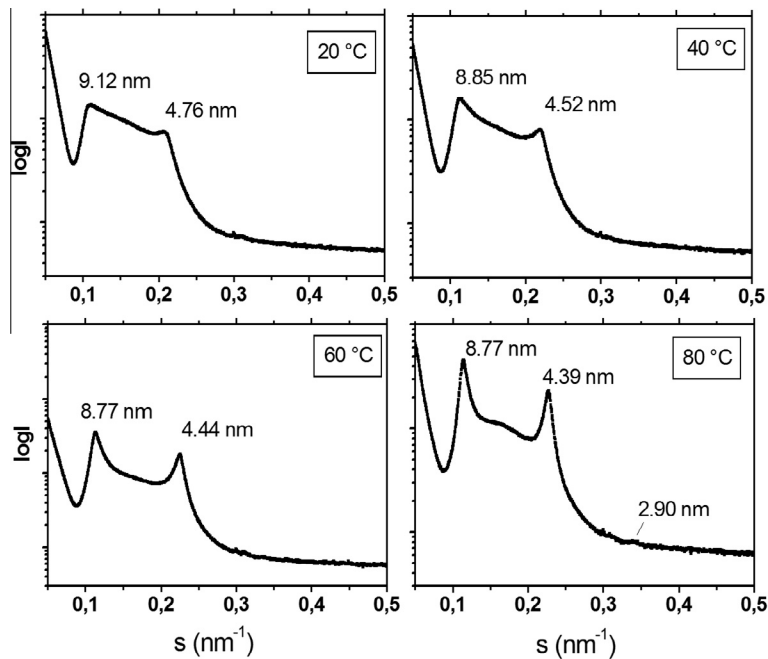


**Fig. 6.** Small-angle X-ray scattering (SAXS) of a [LPS]:[ $\beta_2$ GPI] 1:4 weight% dispersion at 20–80 °C. The logarithm of the scattering intensity  $\log I$  is plotted versus the scattering vector  $s (=1/d, d = \text{spacings of the reflections})$ .

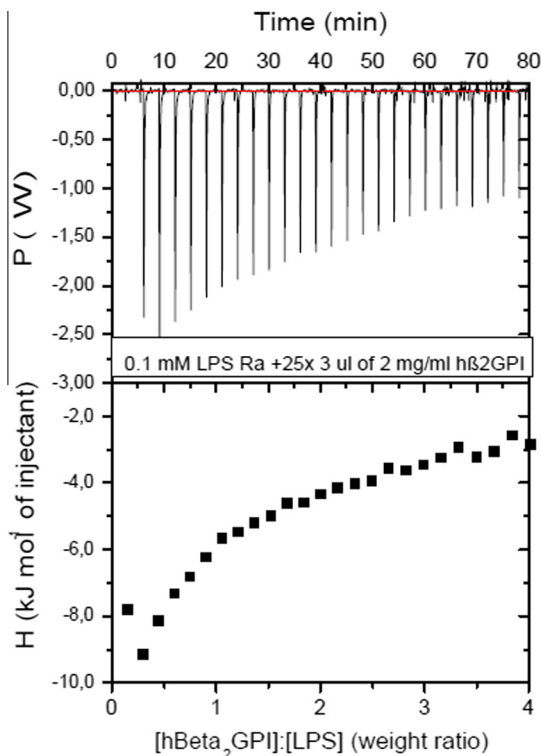


**Fig. 7.** Isothermal titration calorimetric experiments of LPS protein mixtures. To a LPS dispersion (1 mM),  $\beta_2$ GPI (2 mg/ml) is titrated in 3  $\mu$ l portions. Measurements were done at 37 °C. Exothermic processes lead to negative, endothermic processes to positive enthalpy changes  $\Delta H_c$ .

do not give a satisfactory picture for an understanding of the complex behavior of  $\beta_2$ GPI alone and in the presence of different lipids. Therefore further detailed analyzes of the interaction of the protein with the most important lipid systems deserve closer attention.

Agar and co-workers published data from which they deduced that  $\beta_2$ GPI belongs to the class of defensive proteins by scavenging

LPS [7]. These data result among others from the inhibition of the LPS-induced production of tissue factor and interleukin-6 in monocytes. In contrast to this hypothesis our data do not favor an important role of  $\beta_2$ GPI as defense structure. Biophysical data of other defense structures such as polymyxin B [22], high-density lipoprotein [23], lactoferrin [24] and various antimicrobial peptides [25] indicate a much higher change of LPS membrane fluidity leading in most cases to complete fluidization, considerably higher multilamellarization of the LPS aggregates and a much higher exothermic reaction in the ITC experiments with starting values of 80 kJ/mol and with saturation characteristics. Furthermore the decrease of the LPS-induced immunostimulatory activity elicited by the protein in the range [LPS]:[ $\beta_2$ GPI] 1:1–1:100 weight% shown in Fig. 1 is much lower than for the defense proteins and peptides described above [18–21].

The weak and non-saturable binding of  $\beta_2$ GPI to LPS – resembling a catalysis-like process, but not necessarily being catalytic – could be a signal of an immune modulating function of the protein. This view is supported by FRET data (Fig. 8B) and is in accordance with the strong interaction of  $\beta_2$ GPI with phosphatidylserine (PS) as reported earlier [18]. In this work a direct interaction of the positively charged lysine-rich region of  $\beta_2$ GPI with the PS head group was suggested. As also presented in our work PS is an important phospholipid compound in the context of apoptotic processes. Thereby PS is exported from the inner monolayer of immune cells to its outer side thereby being directly accessible to the action of  $\beta_2$ GPI. In this sense we would agree with the statement of Agar et al. [7] that  $\beta_2$ GPI could play a role as component of innate immunity. Regarding their data of cytokine inhibition however, which is only moderate even at rather high excess of  $\beta_2$ GPI with respect to LPS we would not support the view that  $\beta_2$ GPI has a significant role for LPS neutralization and clearance. The interpretation of an immune modulating property of  $\beta_2$ GPI seems also to be in accordance with data of Ninivaggi et al. [26] who found that  $\beta_2$ GPI incubated with phospholipids inhibited the generation of thrombin.

Laplante et al. [6] also investigated the interaction of  $\beta_2$ GPI with LPS. They reported that  $\beta_2$ GPI interacts specifically with LPS and that this interaction is responsible for apparent TLR4 activation

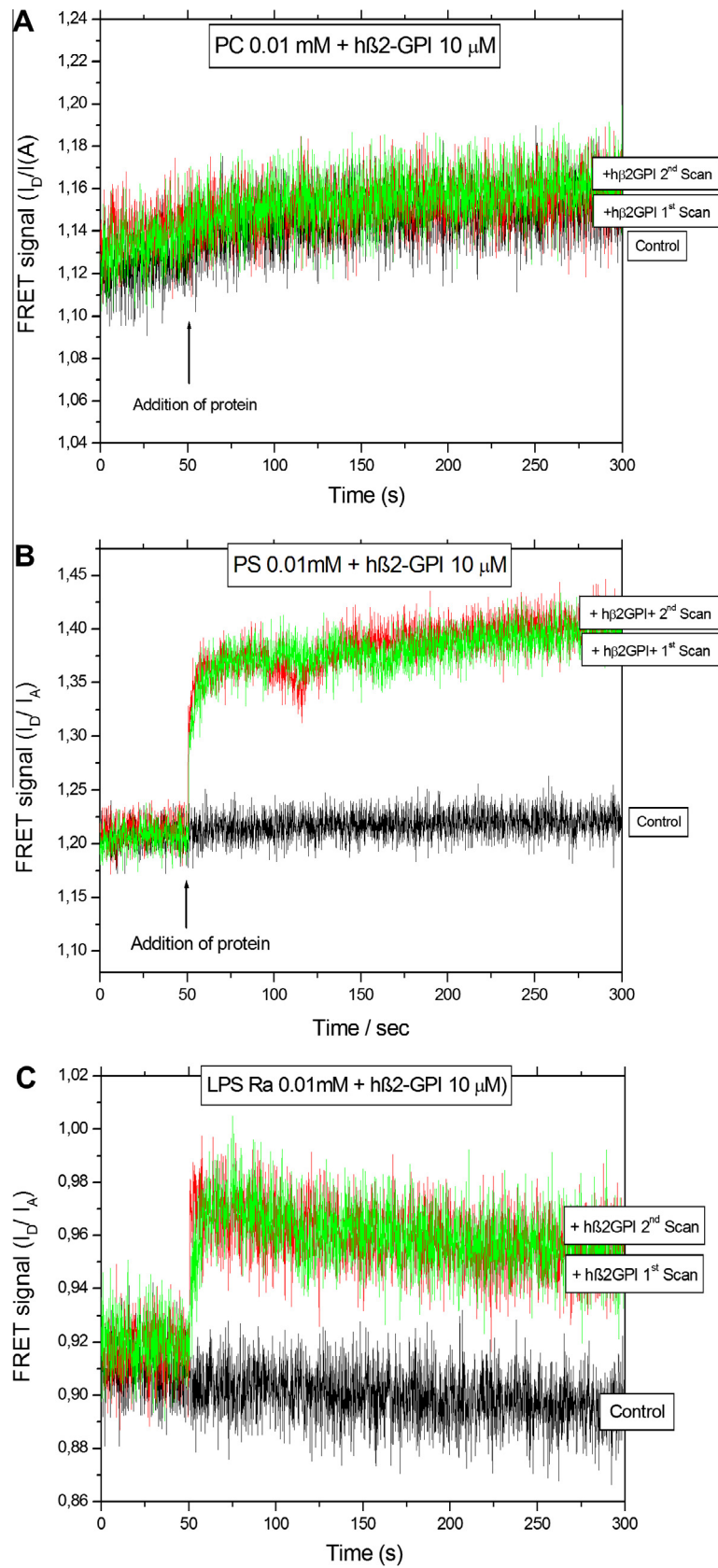


**Fig. 8.** Förster resonance energy transfer spectroscopy (FRET) of mixtures from doubly labeled 0.01 mM phosphatidylcholine (A), phosphatidylserine (B) and LPS Ra (C) with  $\beta_2$ GPI (10  $\mu$ M) added after 50 s. The FRET signal  $I_D/I_A$  is a sensitive measure of incorporation of the protein into the lipids.



by  $\beta_2$ GPI. We do not agree that (i) the binding of  $\beta_2$ GPI to LPS is specific (see above) and (ii) there is a significant interaction of  $\beta_2$ GPI with TLR4. Laplante et al. were unable to prove the latter interaction because they found no immune stimulatory action of  $\beta_2$ GPI in cases when the contaminating LPS was removed by purification or by polymyxin B. Thus, their statement that 'both LPS and TLR4 are required for  $\beta_2$ GPI to bind to and activate macrophages' remains not fully supported.

Further experiments seem to be necessary to elucidate the interaction of  $\beta_2$ GPI with LPS and other negatively charged lipids from different membranes. Particularly atomic force microscopy should be applied to give a view on the immune cell's membrane to explain the direct interaction of  $\beta_2$ GPI and  $\beta_2$ GPI:LPS mixtures with the membrane and its components, in particular with phosphatidylserine.

### Acknowledgements

We kindly acknowledge the help of Nina Hahlbrock and Christine Hamann for performing the IR spectroscopic and cytokine as well as the FRET experiments. The technical assistance of Josef Kellner is also gratefully acknowledged.

We are indebted to the German Ministry (Ministerium für Bildung und Forschung) BMBF, project 01GU0824 and the Else Kröner-Fresenius-Stiftung, project 2011\_A140 for financial help.

### References

- [1] Tapping, R.I., Gegner, J.A., Kravchenko, V.V. and Tobias, P.S. (1998) Roles for LBP and soluble CD14 in cellular uptake of LPS. *Prog. Clin. Biol. Res.* 397, 73–78.
- [2] Ellass-Rochard, E., Legrand, D., Salmon, V., Roseanu, A., Trif, M., Tobias, P.S., Mazurier, J. and Spik, G. (1998) Lactoferrin inhibits the endotoxin interaction with CD14 by competition with the lipopolysaccharide-binding protein. *Infect. Immun.* 66, 486–491.
- [3] Schwarzenbacher, R., Zeth, K., Diederichs, K., Gries, A., Kostner, G.M., Laggner, P. and Prassl, R. (1999) Crystal structure of human beta2-glycoprotein I: implications for phospholipid binding and the antiphospholipid syndrome. *EMBO J.* 18, 6228–6239.
- [4] Bouma, B., de Groot, P.G., van Den Elsen, J.M., Ravelli, R.B., Schouten, A., Simmelink, M.J., Derksen, R.H., Kroon, J. and Gros, P. (1999) Adhesion mechanism of human beta(2)-glycoprotein I to phospholipids based on its crystal structure. *EMBO J.* 18, 5166–5174.
- [5] Hammel, M., Schwarzenbacher, R., Gries, A., Kostner, G.M., Laggner, P. and Prassl, R. (2001) Mechanism of the interaction of beta(2)-glycoprotein I with negatively charged phospholipid membranes. *Biochemistry* 40, 14173–14181.
- [6] Laplante, P., Amireault, P., Subang, R., Dieude, M., Levine, J.S. and Rauch, J. (2011) Interaction of beta2-glycoprotein I with lipopolysaccharide leads to Toll-like receptor 4 (TLR4)-dependent activation of macrophages. *J. Biol. Chem.* 286, 42494–42503.
- [7] Agar, C., de Groot, P.G., Morgelin, M., Monk, S.D., van Os, G., Levels, J.H., de Laat, B., Urbanus, R.T., Herwald, H., van der, P.T. and Meijers, J.C. (2011) Beta(2)-glycoprotein I: a novel component of innate immunity. *Blood* 117, 6939–6947.
- [8] Alexander, C. and Rietschel, E.T. (2001) Bacterial lipopolysaccharides and innate immunity. *J. Endotoxin Res.* 7, 167–202.
- [9] Galanos, C., Luderitz, O. and Westphal, O. (1969) A new method for the extraction of R lipopolysaccharides. *Eur. J. Biochem.* 9, 245–249.
- [10] Gries, A., Nimpf, J., Wurm, H., Kostner, G.M. and Kenner, T. (1989) Characterization of isoelectric subspecies of asialo-beta 2-glycoprotein I. *Biochem. J.* 260, 531–534.
- [11] Heinbockel, L., Sanchez-Gomez, S., Martinez, D.T., Domming, S., Brandenburg, J., Kaconis, Y., Hornef, M., Dupont, A., Marwitz, S., Goldmann, T., Ernst, M., Gutsmann, T., Schurholz, T. and Brandenburg, K. (2013) Preclinical investigations reveal the broad-spectrum neutralizing activity of peptide Pep19-2.5 on bacterial pathogenicity factors. *Antimicrob. Agents Chemother.* 57, 1480–1487.
- [12] Roessle, M.W., Klaering, R., Ristau, U., Robrahn, B., Jahn, D., Gehrman, T., Konarev, P., Round, A., Fiedler, S., Hermes, C. and Svergun, D. (2007) Upgrade of the small-angle X-ray scattering beamline X33 at the European Molecular Biology Laboratory, Hamburg. *J. Appl. Crystallogr.* 40, S190–S194.
- [13] Kaconis, Y., Kowalski, I., Howe, J., Brauser, A., Richter, W., Razquin-Olazarán, I., Inigo-Pestana, M., Garidel, P., Rössle, M., Martínez de Tejada, G., Gutsmann, T. and Brandenburg, K. (2011) Biophysical mechanisms of endotoxin neutralization by cationic amphiphilic peptides. *Biophys. J.* 100, 2652–2661.
- [14] Brandenburg, K. and Seydel, U. (1998) Infrared spectroscopy of glycolipids. *Chem. Phys. Lipids* 96, 23–40.
- [15] Mantsch, H.H. and Chapman, D. (1996) *Infrared Spectroscopy of Biomolecules*, Wiley Press, New York.
- [16] Sanghera, D.K., Wagenknecht, D.R., McIntyre, J.A. and Kamboh, M.I. (1997) Identification of structural mutations in the 5th domain of apolipoprotein H(beta-2-glycoprotein-I) which affect phospholipid-binding. *Hum. Mol. Genet.* 6, 311–316.
- [17] Horbach, D.A., Vanoort, E., Tempelman, M.J., Derksen, R.H.W.M. and Degroot, P.G. (1998) The prevalence of a non-phospholipid-binding form of beta(2)-glycoprotein I in human plasma. *Thromb. Haemost.* 80, 791–797.
- [18] Gamsjaeger, R., Johs, A., Gries, A., Gruber, H.J., Romanin, C., Prassl, R. and Hinterdorfer, P. (2005) Membrane binding of beta2-glycoprotein I can be described by a two-state reaction model: an atomic force microscopy and surface plasmon resonance study. *Biochem. J.* 389, 665–673.
- [19] Rappolt, M., Rössle, M., Kaconis, Y., Howe, J., Andra, J., Gutsmann, T. and Brandenburg, K. (2011) X-ray scattering of bacterial cell wall compounds and their neutralization in: X-ray Scattering (Bauwens, C., Ed.), pp. 133–148, NOVA Science Publisher, Hauppauge, NY.
- [20] Paolrossi, M. and Montich, G.G. (2011) Conformational changes of beta2-human glycoprotein I and lipid order in lipid-protein complexes. *Biochim. Biophys. Acta* 1808, 2167–2177.
- [21] Borchman, D., Harris, E.N., Pierangeli, S.S. and Lamba, O.P. (1995) Interactions and molecular structure of cardiolipin and beta 2-glycoprotein 1 (beta 2-GP1). *Clin. Exp. Immunol.* 102, 373–378.
- [22] Brandenburg, K., Moriyo, I., Arraiza, M.D., Lewark-Yvetot, G., Koch, M.H.J. and Seydel, U. (2002) Biophysical investigations into the interaction of lipopolysaccharide with polymyxins. *Thermochim. Acta* 382, 189–198.
- [23] Brandenburg, K., Jurgens, G., Andra, J., Lindner, B., Koch, M.H., Blume, A. and Garidel, P. (2002) Biophysical characterization of the interaction of high-density lipoprotein (HDL) with endotoxins. *Eur. J. Biochem.* 269, 5972–5981.
- [24] Brandenburg, K., Jurgens, G., Muller, M., Fukuoka, S. and Koch, M.H. (2001) Biophysical characterization of lipopolysaccharide and lipid A inactivation by lactoferrin. *Biol. Chem.* 382, 1215–1225.
- [25] Andra, J., Howe, J., Garidel, P., Rössle, M., Richter, W., Leiva-Leon, J., Moriyo, I., Bartels, R., Gutsmann, T. and Brandenburg, K. (2007) Mechanism of interaction of optimized Limulus-derived cyclic peptides with endotoxins: thermodynamic, biophysical and microbiological analysis. *Biochem. J.* 406, 297–307.
- [26] Ninivaggi, M., Kelchtermans, H., Lindhout, T. and de Laat, B. (2012) Conformation of beta2glycoprotein I and its effect on coagulation. *Thromb. Res.* 130 (Suppl. 1), S33–S36.